

3. Enting, I. G., Wigley, T. M. L. & Heimann, M. *Future Emissions and Concentrations of Carbon Dioxide: Key Ocean/Atmosphere/Land Analyses* (CSIRO Division of Atmospheric Research, 31, 1994).
4. Sarmiento, J. L., Le Quéré, C. & Pacala, S. W. Limiting future atmospheric carbon dioxide. *Glob. Biogeochem. Cycles* **9**, 121–138 (1995).
5. Haywood, J. M., Stouffer, R. J., Wetherald, R. T., Manabe, S. & Ramaswamy, V. Transient response of a coupled model to estimate changes in greenhouse gas and sulfate concentrations. *Geophys. Res. Lett.* **24**, 1335–1338 (1997).
6. Manabe, S. & Stouffer, R. J. Century-scale effects of increased atmospheric CO₂ on the ocean–atmosphere system. *Nature* **364**, 215–218 (1993).
7. Manabe, S., Stouffer, R. J., Spelman, M. J. & Bryan, K. Transient responses of a coupled ocean–atmosphere model to gradual changes of atmospheric CO₂. Part 1: annual mean response. *J. Clim.* **7**, 85–118 (1994).
8. Sarmiento, J. L. & Le Quéré, C. Oceanic carbon dioxide uptake in a model of century-scale global warming. *Science* **274**, 1346–1350 (1996).
9. Coale, K. H. *et al.* A massive phytoplankton bloom induced by an ecosystem-scale iron fertilization experiment in the equatorial Pacific Ocean. *Nature* **383**, 495–501 (1996).
10. Johnson, K. S., Gordon, R. M. & Coale, K. H. What controls dissolved iron concentrations in the world ocean? *Mar. Chem.* **57**, 137–161 (1997).
11. Sarmiento, J. L. & Orr, J. C. Three-dimensional simulations of the impact of Southern Ocean nutrient depletion on atmospheric CO₂ and ocean chemistry. *Limnol. Oceanogr.* **36**, 1928–1950 (1991).
12. Siegenthaler, U. & Wenk, T. Rapid atmospheric CO₂ variations and ocean circulation. *Nature* **308**, 624–626 (1984).
13. Sarmiento, J. L. & Toggweiler, J. R. A new model for the role of the oceans in determining atmospheric pCO₂. *Nature* **380**, 621–624 (1984).
14. Knox, F. & McElroy, M. Changes in atmospheric CO₂, influence of marine biota at high latitudes. *J. Geophys. Res.* **89**, 4629–4637 (1984).
15. Sarmiento, J. L., Orr, J. C. & Siegenthaler, U. A perturbation simulation of CO₂ uptake in an ocean general circulation model. *J. Geophys. Res.* **97**, 3621–3646 (1992).
16. Manabe, S. & Stouffer, R. J. Multiple century response of a coupled ocean–atmosphere model to an increase of atmospheric carbon dioxide. *J. Clim.* **7**, 5–23 (1994).
17. Maier-Reimer, E., Mikolajewicz, U. & Winguth, A. Future ocean uptake of CO₂: interaction between ocean circulation and biology. *Clim. Dyn.* **12**, 711–721 (1996).
18. Gent, P. R., Willebrand, J., McDougall, T. J. & McWilliams, J. C. Parameterizing eddy-induced tracer transports in ocean circulation models. *J. Phys. Oceanogr.* **25**, 463–474 (1995).
19. Denman, K., Hofmann, E. & Marchant, H. In *Climate Change 1995* (ed. Houghton, J. T.) 483–516 (Cambridge Univ. Press, 1996).
20. Keeling, R. F., Najjar, R. P., Bender, M. L. & Tans, P. P. What atmospheric oxygen measurements can tell us about the global carbon cycle. *Glob. Biogeochem. Cycles* **7**, 37–68 (1993).
21. Bender, M., Ellis, T., Tans, P., Francey, R. & Lowe, D. Variability in the O₂/N₂ ratio of southern hemisphere air, 1991–1994: implications for the carbon cycle. *Glob. Biogeochem. Cycles* **10**, 9–22 (1996).
22. Mitchell, J. F. B., Johns, T. C., Gregory, J. M. & Tett, S. F. B. Climate response to increasing levels of greenhouse gases and sulphate aerosols. *Nature* **376**, 501–504 (1995).
23. Houghton, J. T., Callander, B. A. & Varney, S. K. (eds) *Climate Change 1992* (Cambridge Univ. Press, 1992).
24. Sarmiento, J. L., Murnane, R. & Quéré, C. L. Air–sea CO₂ transfer and the carbon budget budget of the North Atlantic. *Phil. Trans. R. Soc. Lond. B* **348**, 211–218 (1995).
25. Martin, J. H., Knauer, G. A., Karl, D. M. & Broenkow, W. W. VERTEX: carbon cycling in the northeast Pacific. *Deep-Sea Res.* **34**, 267–285 (1987).
26. Wanninkhof, R. Relationship between wind speed and gas exchange over the ocean. *J. Geophys. Res.* **97**, 7373–7383 (1992).
27. Archer, D., Kheshti, H. & Maier-Reimer, E. Multiple timescales for the neutralization of fossil fuel CO₂. *Geophys. Res. Lett.* **24**, 405–408 (1997).

Acknowledgements. We thank Corinne Le Quéré for adding the carbon component of the coupled model, Fortunat Joos for providing the atmospheric CO₂ figures, and Jerry Mahlman and Yasuhiro Yamamoto, as well as Klaus Keller, Francois Morel, Philippe Tortell and Ernst Maier-Reimer, for comments. The contributions of J.L.S. and T.M.C.H. were supported by the Office of Global Programs of the National Oceanic and Atmospheric Administration, and by the National Science Foundation. The paper was written in part while J.L.S. was visiting the Bermuda Biological Station for Research with support from EXXON Corporation; J.L.S. thanks Tony Knap for making the arrangements.

Correspondence and requests for materials should be addressed to J.L.S. (e-mail: jls@splash.princeton.edu).

Dynamic responses of terrestrial ecosystem carbon cycling to global climate change

Mingkui Cao* & F. Ian Woodward

Department of Animal and Plant Sciences, University of Sheffield, Sheffield S10 2TN, UK

Terrestrial ecosystems and the climate system are closely coupled, particularly by cycling of carbon between vegetation, soils and the atmosphere. It has been suggested^{1,2} that changes in climate and in atmospheric carbon dioxide concentrations have modified the carbon cycle so as to render terrestrial ecosystems as substantial

carbon sinks^{3,4}; but direct evidence for this is very limited^{5,6}. Changes in ecosystem carbon stocks caused by shifts between stable climate states have been evaluated^{7,8}, but the dynamic responses of ecosystem carbon fluxes to transient climate changes are still poorly understood. Here we use a terrestrial biogeochemical model⁹, forced by simulations of transient climate change with a general circulation model¹⁰, to quantify the dynamic variations in ecosystem carbon fluxes induced by transient changes in atmospheric CO₂ and climate from 1861 to 2070. We predict that these changes increase global net ecosystem production significantly, but that this response will decline as the CO₂ fertilization effect becomes saturated and is diminished by changes in climatic factors. Thus terrestrial ecosystem carbon fluxes both respond to and strongly influence the atmospheric CO₂ increase and climate change.

Ecosystem carbon fluxes are controlled by the processes of photosynthesis, plant (autotrophic) respiration and soil (heterotrophic) respiration. The difference between plant photosynthesis and respiration is defined as net primary production (NPP), and the difference between NPP and soil respiration, defined as net ecosystem production (NEP), represents the net carbon flux from the atmosphere to ecosystems. Among many factors affecting these processes, the most obvious at the global scale are elevated CO₂ concentration and climate change, which directly and indirectly influence and interact to control the carbon fluxes from ecological and physiological processes^{1,2}. We have used the carbon exchange between vegetation, soil and the atmosphere (CEVSA) model⁹ to assess the dynamic responses of natural terrestrial ecosystems to CO₂ increases and climate change from the onset of industrialization (the 1860s) to a doubling of current radiative forcing, which will be reached in the 2060s based on IPCC scenario IS92a (ref. 11). The model simulates the processes of stomatal conductance, evapotranspiration, plant photosynthesis and respiration, nitrogen uptake, carbon allocation among plant organs, litter production, nitrogen mineralization and soil organic carbon decomposition, and uses these to calculate the carbon fluxes between vegetation, soils and the atmosphere. We do not include the effects of nitrogen deposition and modifications to ecosystem structure and distribution by natural and anthropogenic processes.

The scenarios of transient CO₂ concentration and climate change between 1861 and 2070 used in this study were produced by the Hadley Centre for Climate Prediction and Research, UK Meteorological Office with a coupled ocean–atmospheric general circulation model (GCM), which accounts for the effects of both greenhouse gases and aerosols^{10,12}. The concentrations of greenhouse gases and aerosols used by the GCM for the period 1861–1990 were derived from observed data, whereas those after 1990 were based on IPCC scenario IS92a with an increase in CO₂ by 1% yr^{−1} (ref. 11). This climate projection has been appropriately tested against observed trends and spatial patterns of climate^{10,12}.

We use the CEVSA model and the GCM scenarios of CO₂ and climate change to make simulations at a spatial resolution of 2.5° latitude × 3.75° longitude and a time step of one month. The model is first run with the GCM simulation of pre-industrial climate until an ecological equilibrium is reached, that is when the differences between annual NPP, litter production and soil respiration, and the interannual variations in soil moisture and carbon stocks were less than 0.1%. After reaching this equilibrium, the model is driven by the GCM simulation of the transient changes in CO₂ and climate from 1861 to 2070.

We isolated and combined the effects of elevated CO₂ and climate change by simulations with CO₂ increase but no climate change, climate change but no CO₂ increase, and both CO₂ increase and climate change. In addition to a global-scale analysis, the results are integrated into three latitudinal zones, northern (>40° N), temperate (40° N–20° N and >30° S) and tropical (20° N–30° S)

* Present address: Department of Environmental Sciences, University of Virginia, Charlottesville, Virginia 22903, USA.

ecosystems, to investigate the differential responses among climate–vegetation regions.

The scenarios of CO₂ increase and climate change and a comparison between the simulated and observed¹³ temperature are shown in Fig. 1. Between the 1860s and the 2060s, CO₂ increases from 288 to 640 p.p.m.v., global terrestrial temperature rises from 12.5 to 15.5 °C and annual precipitation changes little globally but increases by 9% in northern ecosystems and decreases by 4% in temperate and tropical ecosystems. The changes in climate are predicted to cause decreases in soil moisture from the 1960s (Fig. 1). In northern ecosystems increases in precipitation counteract the drying effect of warming and soil moistures change little. By contrast, in temperate and tropical ecosystems, soil moisture decreases by 10% and 8%, respectively, because of the warming and decrease in precipitation.

NPP, NEP and carbon stocks are predicted to increase substantially under CO₂ increase but no climate change (Fig. 2a). Over the period 1861–2070 NPP increases by 45% in tropical ecosystems, 36% in northern ecosystems and 20% in temperate ecosystems. Carbon stocks increase by 185 Gt in northern ecosystems, 105 Gt in temperate ecosystems and 200 Gt in tropical ecosystems. The strongest CO₂ fertilization on NPP in the tropics correlates with the largest increase in water-use efficiency. As CO₂ increases from 288 to 640 p.p.m.v., stomatal conductance and evapotranspiration in tropical ecosystems decrease by 19% and 6%, respectively,

and water-use efficiency increases by 56%. In contrast, stomatal conductance decreases by only 13% and evapotranspiration changes little in temperate and northern ecosystems, however, the water-use efficiency still increases by 31% and 42%, respectively.

Globally, the CO₂ fertilization effect is found to decrease as

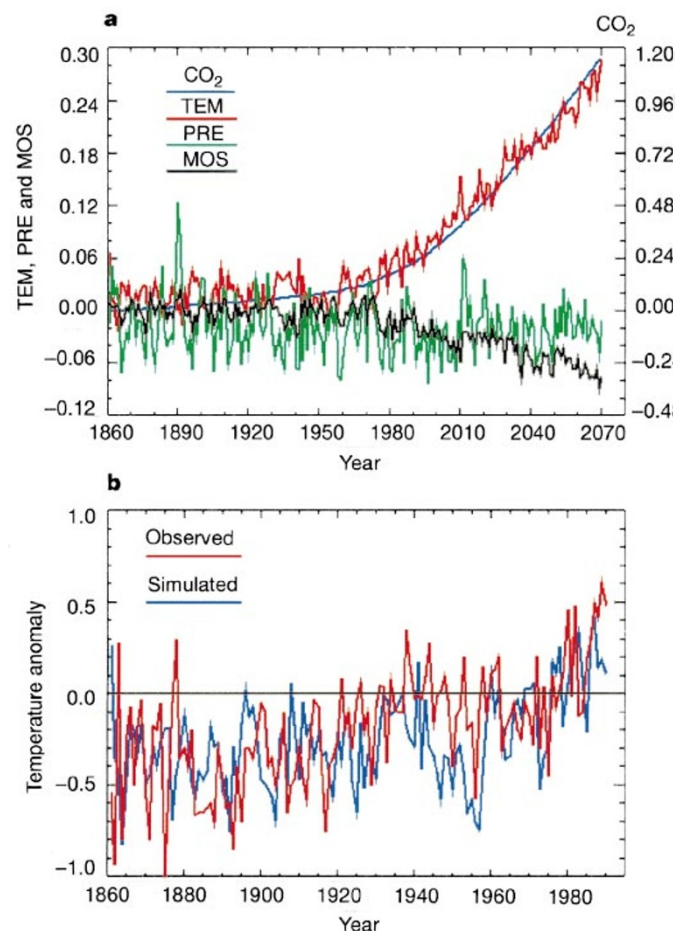


Figure 1 The scenarios. **a**, The GCM scenarios of atmospheric CO₂ and climate change¹⁰ used in this study and our simulated variation in soil moisture. All values represent the proportional changes relative to the averages in the period 1840–1880, which are 288 p.p.m.v. for atmospheric CO₂, 12.5 °C for annual mean terrestrial temperature (TEM), 805 mm for annual precipitation (PRE) and 0.51 (relative to soil water holding capacity) for soil moisture (MOS). **b**, A comparison between the GCM simulated and observed anomaly¹³ in global-mean terrestrial temperature (°C).

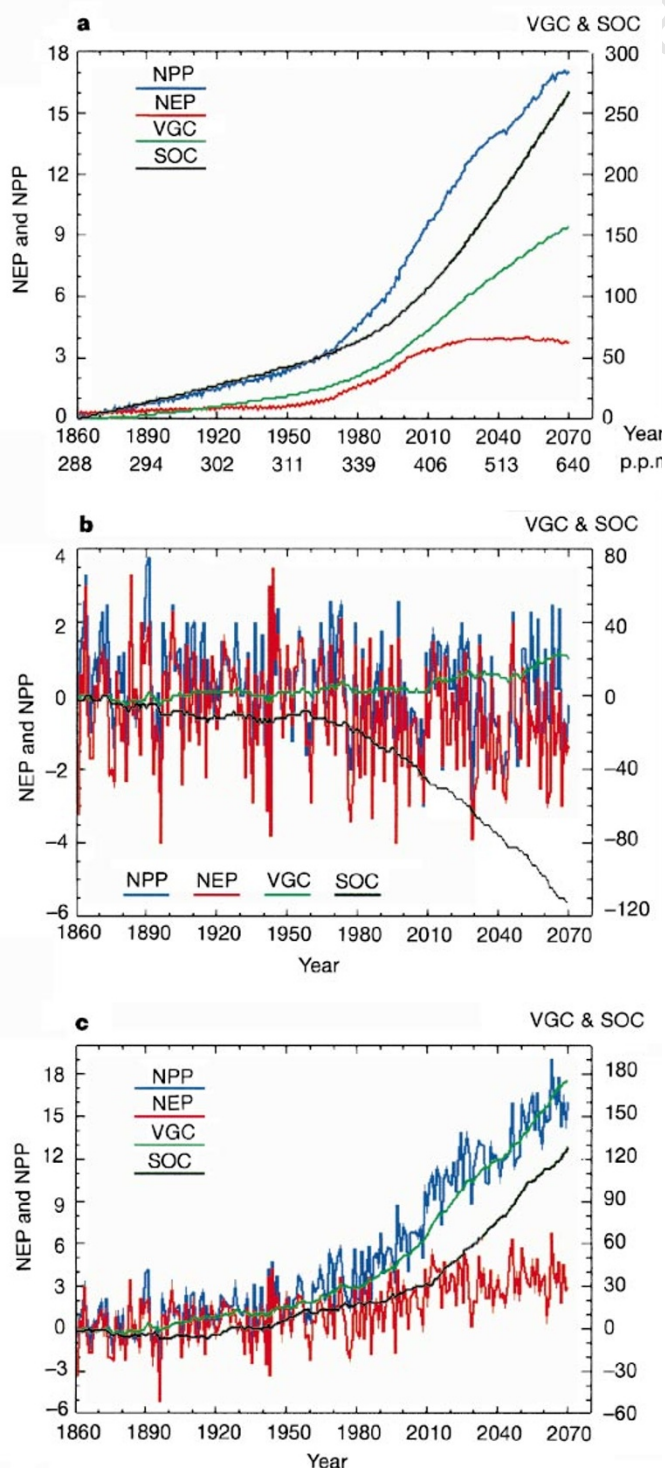


Figure 2 The variations in global net primary production (NPP, Gt C yr⁻¹), net ecosystem production (NEP, Gt C yr⁻¹), and carbon stocks in vegetation (VGC, Gt C) and soils (SOC, Gt C) resulting from atmospheric CO₂ increase and climate change. The initial values are 45 Gt C yr⁻¹ for NPP, zero for NEP, 441 Gt C for VGC, and 1238 Gt C for SOC. **a**, CO₂ increase only; **b**, climate change only; **c**, CO₂ increase and climate change.

CO₂ increases (Fig. 2a); the relative NPP enhancement decreases markedly as CO₂ exceeds 500 p.p.m.v., and NEP saturates at a CO₂ concentration of 450 p.p.m.v. The stimulation of photosynthesis by elevated CO₂ diminishes at high CO₂ concentration, but respiration increases as carbon accumulates in vegetation and soils. If CO₂ increases continually, NPP is predicted to saturate at a CO₂ concentration of about 1,200 p.p.m.v., and NEP declines as CO₂ exceeds 600 p.p.m.v. (Fig. 3). If CO₂ is stabilized, NEP falls rapidly and eventually reaches zero (Fig. 3), because photosynthesis will be balanced by increased plant and soil respiration.

Under climate change with no CO₂ increase, we predict wide interannual fluctuations in the carbon fluxes (Fig. 2b) and differential responses among various ecosystems. In northern ecosystems, NPP is enhanced by 13% and vegetation carbon stocks are increased by 28 Gt C in the period 1861–2070, however, soil carbon stocks are reduced by 55 Gt C at the same time because soil respiration is stimulated by warming. NEP is predicted to decrease to –0.2 Gt C yr^{–1} in the 1980s, and to –0.5 Gt C yr^{–1} in the 2060s. In temperate ecosystems NPP and NEP are slightly reduced with a total loss of 8 Gt C between 1861 and 2070. In tropical ecosystems, NPP is reduced by 6% and NEP is decreased to about –0.4 Gt C yr^{–1} from the 1970s, leading to a total loss of 52 Gt C in the period 1861–2070.

Climate change has little effect on global NPP, the increase in the north offsets the decrease in the tropics. However, global NEP is decreased to –0.4 Gt C yr^{–1} in the period 1951–2000, and to –0.8 Gt C yr^{–1} in the period 2001–2070, consistent with a predicted global reduction in soil moisture (Fig. 1a). Although vegetation carbon stocks are increased slightly, soil carbon stocks are reduced markedly (Fig. 2b). The total carbon stocks decrease by 87 Gt from 1861 to 2070 because of stronger increases in soil respiration than NPP in the north and decreases in NPP in the tropics. This result is supported by estimates that the effect of warming on respiration dominates that on plant growth and reduces soil carbon storage^{14,15}, although it is contrary to some suggestions that climate change has caused a substantial carbon sink^{16,17}. Warming may enhance NPP in the north as suggested by studies^{17,18} based on satellite data of NDVI (the normalized difference vegetation index), but it does not necessarily increase the carbon sink because warming also stimulates soil respiration.

When both CO₂ concentration and climate change, NPP, NEP and carbon stocks all increase (Fig. 2c). From 1861 to 2070 global NPP increases by 36%. Global NEP varies between –6.5 and 5.3 Gt C yr^{–1}, responding positively to changes in CO₂ and precipitation (PRE) but negatively to changes in temperature (TEM) (NEP = 0.036[CO₂] – 2.431TEM + 0.029PRE – 2.868, $r^2 = 0.64$). NEP increases significantly from the 1950s along with the rapid increase

in CO₂, but it steadies after 2020 (Fig. 2c) as the CO₂ fertilization effect saturates (Fig. 2a) and is diminished by climate change (Fig. 2b). The decadal-mean NEP becomes positive from the 1910s and increases to 1.1 Gt C yr^{–1} in the period 1950–1990, and to 3.2 Gt C yr^{–1} in the period 2030–2070. This causes an increase of 309 Gt C in soils and vegetation from 1861 to 2070, in contrast with an increase of 490 Gt C under CO₂ increase and a loss of 87 Gt C under climate change alone.

Increases in CO₂ and temperature interact positively to enhance NPP in the north, whereas elevated CO₂ reverses the decreases in NPP caused by climate change in the tropics. Marked increases in NEP therefore occur in both the tropics and the north under combined changes in CO₂ and climate (Fig. 4a). The NEPs in the north and tropics are of a similar magnitude under the contemporary climate, but NEPs in the north will become much higher than in the tropics in the future (Fig. 4a) because the strongest NPP increase is predicted to occur at northern high latitudes. Although various evidence supports a substantial carbon sink in the north, data confirming a tropical carbon sink are limited^{3,4}. Direct measurements and modelling of CO₂ fluxes^{6,19} show that tropical ecosystems are taking up carbon; however, the carbon sink may be concealed by the carbon release from deforestation⁴.

Climate change and elevated CO₂ also modify seasonal ecosystem carbon fluxes. NEP increases between May and September but decreases in other months, its seasonal amplitude is therefore greatly amplified (Fig. 4b). This variation is mainly due to the changes occurring in the north: the increase in soil respiration is higher than in NPP in winter and spring but is lower in summer. Strong increases in soil respiration by warming in winter and spring have been observed^{20,21}. In summer, the advantage of increased

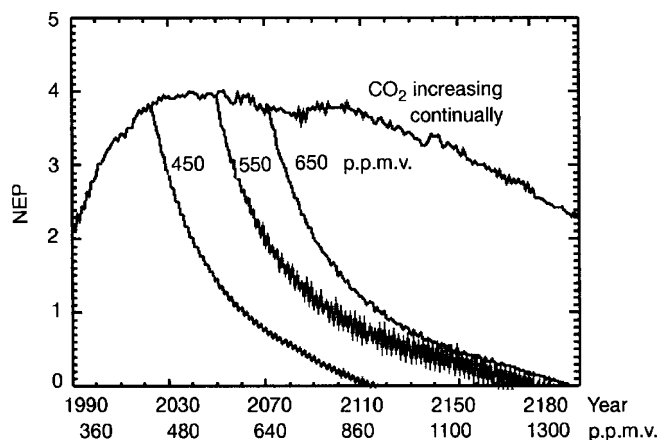


Figure 3 Variations in global net ecosystem production (NEP, Gt C yr^{–1}) responding to stabilization of atmospheric CO₂ at 450, 550 and 650 p.p.m.v., or continual increase. This estimate is made with changes in atmospheric CO₂ only.

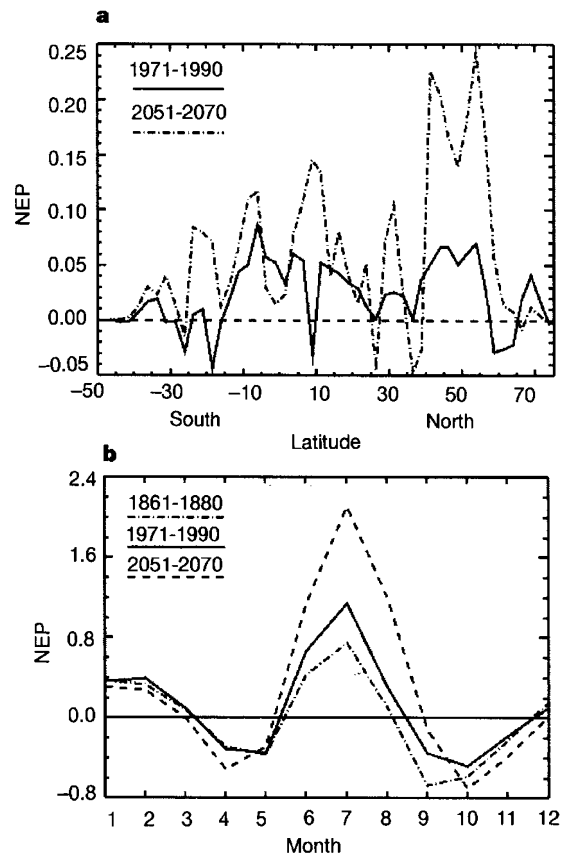


Figure 4 Spatial and seasonal variations in net ecosystem production (NEP) in response to atmospheric CO₂ increase and climate change. **a**, Latitudinal distributions in NEP (Gt C yr^{–1}) in the periods 1971–1990 and 2051–2070. All values represent that for the land in 2.5° latitudinal bands. **b**, Seasonal change in global NEP (Gt C month^{–1}) in the periods 1861–1880, 1971–1990 and 2051–2070.

temperature and CO₂ to NPP can be fully utilized because precipitation is plentiful and leaf canopies are fully expanded.

A consequence of CO₂ increase and climate change is that global terrestrial ecosystems are estimated to have sequestered 58 Gt C in the period 1861–1990, accounting for about two-thirds of the unattributed terrestrial biospheric sink from deconvolutions²². Forest regrowth^{23,24} and nitrogen deposition^{7,25} also contribute to the terrestrial carbon sink, although estimates of these sinks are particularly uncertain. Forests accumulate carbon in young and middle age, but the rates decline to zero as stands mature. A full inventory of forest demographic changes is essential to estimate the carbon sinks caused by forest regrowth. Although disturbance by human (such as harvest and management) and natural factors (such as fire and wind) initially stimulate forest growth^{23,24}, decreased nutrient availability and increased stomatal limitation cause a decline in NPP as stands age²⁶. Nitrogen is the primary nutrient that limits both plant production and soil decomposition⁹ and often constrains CO₂ fertilization²⁷. Plants may acclimatize to nitrogen supply by adjusting nitrogen allocation among organs and biomass distribution between under- and aboveground^{7,27}. These mechanisms are central to estimates of the effect of nitrogen deposition and the interaction with elevated CO₂, but little is known at present. It is important to recognize also that changes in CO₂ and climate may cause transient changes in vegetation composition and distribution²⁸, but this effect is not included in this study. The sensitivity of vegetation to CO₂ concentration and climate varies with plant species and stand age^{26,28}, and rapid climate change can cause the die back of some vegetation types and consequent carbon loss before new types are established⁸. Models simulating ecosystem structure dynamics are being developed to assess the effects of demographic and compositional changes of forests^{29,30}.

We predict that the net effect of CO₂ increase and climate change is to increase global NEP substantially, but that the response of natural terrestrial ecosystems depends largely upon changes in individual factors and varies widely among climate-vegetation zones. This information is critical for calculations of CO₂ stabilization and new developments in GCMs, in which the feedback of ecosystem carbon cycling on CO₂ have not yet been taken into account. The dynamic simulation of ecosystem carbon fluxes in this study, along with progress in understanding the effect of nitrogen deposition and transient changes in ecosystem structure, will lead to a full coupling between ecosystem carbon processes and climatic systems that is essential for more realistic predictions of both ecosystem responses and climate change. □

Received 5 June 1997; accepted 16 March 1998.

1. Amthor, J. S. Terrestrial higher-plant response to increasing atmospheric [CO₂] in relation to the global carbon cycle. *Global Change Biol.* **1**, 243–247 (1995).
2. Houghton, R. A. & Woodwell, G. M. Global climatic change. *Sci. Am.* **260**, 36–47 (1989).
3. Ciais, P., Tan, P. P., Troler, M., White, J. W. C. & Francy, R. J. A large northern hemisphere terrestrial CO₂ sink indicated by ¹³C/¹²C of atmospheric CO₂. *Science* **269**, 1098–1102 (1995).
4. Keeling, R. F., Piper, S. C. & Heimann, M. Global and hemispheric CO₂ sinks deduced from changes in atmospheric O₂ concentration. *Nature* **381**, 218–221 (1996).
5. Wofsy, S. C., Munger, J. E., Bakwin, P. S., Daube, B. C. & Moore, T. R. Net CO₂ uptake by northern woodlands. *Science* **260**, 1314–1317 (1993).
6. Grace, J. et al. Carbon dioxide uptake by undisturbed tropical forests, 1992 and 1993. *Science* **270**, 778–780 (1995).
7. Melillo, J. M. in *Global Change and Terrestrial Ecosystems* (eds Walker, B. & Steffen, W.) 431–450 (Cambridge Univ. Press, 1996).
8. Smith, T. M. & Shugart, H. H. The transient response of terrestrial carbon storage to a perturbed climate. *Nature* **361**, 523–526 (1993).
9. Cao, M. K. & Woodward, F. I. Net primary and ecosystem productions and carbon stocks of terrestrial ecosystems and their response to climate change. *Global Change Biol.* **4**, 185–198 (1998).
10. Mitchell, J. F. B., Johns, T. C., Gregory, J. M. & Tett, S. F. B. Climate response to increasing levels of greenhouse gases and sulphate aerosols. *Nature* **376**, 501–504 (1995).
11. Houghton, J. T., Callander, B. A. & Varney, S. K. (eds) *Climate Change 1992. The Supplementary Report to the IPCC Scientific Assessment* (Cambridge Univ. Press, 1992).
12. Johns, T. C. et al. The second Hadley Centre coupled ocean-atmosphere GCM: model description, spinup and validation. *Clim. Dyn.* **13**, 103–134 (1997).
13. Jones, P. D. Hemispheric surface air temperature variations: a reanalysis and an update to 1993. *J. Clim.* **7**, 1794–1802 (1994).
14. Oechel, W. C. et al. Recent change of Arctic tundra ecosystems from a net carbon dioxide sink to a source. *Nature* **361**, 520–523 (1993).
15. Townsend, A. R., Vitousek, P. M. & Holland, E. A. Tropical soils could dominate the short-term carbon cycle feedback to increased global temperature. *Clim. Change* **22**, 293–303 (1992).

16. Dai, A. & Fung, I. Y. Can climate variability contribute to the “missing” CO₂ sink? *Glob. Biogeochem. Cycles* **7**, 599–609 (1993).
17. Braswell, B. H., Schimel, D. S., Linder, E. & Moore, B. The response of global terrestrial ecosystems to interannual temperature variability. *Science* **278**, 870–873 (1997).
18. Myneni, R. B., Keeling, C. D., Tucker, C. J., Asrar, G. & Nemani, R. R. Increased plant growth in the northern high latitudes from 1981 to 1991. *Nature* **386**, 698–702 (1997).
19. Lloyd, J. et al. A simple calibrated model of Amazonian rainforest productivity based on leaf biochemical properties. *Plant Cell Environ.* **18**, 1129–1145 (1995).
20. Oechel, W. C., Vourlitis, G. & Hastings, S. J. Cold season CO₂ emission from Arctic soils. *Glob. Biogeochem. Cycles* **11**, 151–162 (1997).
21. Zimov, S. A. et al. Siberian CO₂ efflux in winter as a CO₂ source and cause of seasonality in atmospheric CO₂. *Clim. Change* **33**, 111–120 (1996).
22. Houghton, R. A. in *The Global Carbon Cycle* (ed. Heimann, M.) 139–157 (Springer, New York, 1993).
23. Dixon, R. K. et al. Carbon pools and flux of global forest ecosystems. *Science* **263**, 185–190 (1994).
24. Melillo, J. M., Frue, P. A., Houghton, R. A., Moore, B. & Skole, D. L. Land-use changes in the Soviet Union between 1850 and 1980: causes of a net release of CO₂ to the atmosphere. *Tellus B* **40**, 116–128 (1988).
25. Holland, E. A. et al. Variations in the predicted spatial distribution of atmospheric nitrogen deposition and their impact on carbon uptake by terrestrial ecosystems. *J. Geophys. Res.* **102**, 15849–15866 (1997).
26. Gower, S. T., McMurtrie, R. E. & Durty, D. Aboveground net primary production decline with stand age: potential causes. *Trends Ecol. Evol.* **11**, 378–383 (1996).
27. McGuire, A. D., Melillo, J. M. & Joyce, L. A. The role of nitrogen in the response of forest net primary production to elevated atmospheric carbon dioxide. *Annu. Rev. Ecol. Syst.* **26**, 473–503 (1995).
28. Schulze, E.-D. Flux control at the ecosystem level. *Trends Ecol. Evol.* **10**, 40–43 (1994).
29. Foley, J. A. et al. An integrated biosphere model of land-surface processes, terrestrial carbon balance, and vegetation dynamics. *Glob. Biogeochem. Cycles* **10**, 603–628 (1996).
30. Pitelka, L. F. et al. Plant migration and climate change. *Am. Sci.* **85**, 464–473 (1997).

Acknowledgements. This work is being supported by the Natural Environment Research Council, UK. We thank R. Betts, the Hadley Centre for Climate Prediction and Research, UK for supplying the climatic and CO₂ data, P. L. Mitchell and D. J. Beerling for their critical comments.

Correspondence and request for materials should be addressed to M.C. (e-mail: mc5m@virginia.edu).

Mineralogy and dynamics of a pyrolite lower mantle

S. E. Kesson, J. D. Fitz Gerald & J. M. Shelley

Research School of Earth Sciences, Australian National University, Canberra ACT 0200, Australia

There is a growing consensus that the Earth's lower mantle possesses a bulk composition broadly similar to that of the upper mantle (known as pyrolite)^{1–3}. But little is known about lower-mantle mineralogy and phase chemistry^{4,5}, especially at depth. Here we report diamond-anvil cell experiments at pressures of 70 and 135 GPa (equivalent to depths within the Earth of about 1,500 and 2,900 km, respectively) which show that pyrolite would consist solely of magnesian-silicate perovskite (MgPv), calcium-silicate perovskite (CaPv) and magnesiowüstite (Mw). Contrary to recent speculation^{6,7}, no additional phases or disproportionations were encountered and MgPv was found to be present at both pressures. Moreover, we estimate that, at ultra-high pressures where thermal expansivities are low, buoyancy forces inherent in subducted slabs because of their lithology will be of similar magnitude to those required for thermally driven upwelling. So slabs would need to be about 850 °C cooler than their surroundings if they are to sink to the base of the mantle. Furthermore, initiation of plume-like upwellings from the core-mantle boundary, long attributed to superheating, may be triggered by lithologically induced buoyancy well before thermal equilibration is attained. We estimate that ascent would commence within ~0.5 Gyr of the slab reaching the core-mantle boundary, in which case the lowermost mantle should not be interpreted as a long-term repository for ancient slabs.

The diamond-anvil cell methodology and its inherent limitations are described in Fig. 1 legend. Our results constrain both the mineralogy and phase chemistry that would be adopted at depth by a pyrolite lower mantle, and cannot substantiate a report⁷ that MgSiO₃ perovskite disproportionates to its component oxides at pressures near 70 GPa. Moreover, existence of the three-phase assemblage of MgPv + Mw + CaPv at ~135 GPa means that no